Available online at www.sciencedirect.com
SCIENCE DIRECT®
Journal of Solid State Chemistry 178 (2005) 2594–2601
JOURNAL OF SOLID STATE CHEMISTRY
www.elsevier.com/locate/jssc

High-pressure synthesis and crystal structure of silicon phosphate hydroxide, $SiPO_4(OH)$

Linda A. Stearns*, Thomas L. Groy, Kurt Leinenweber

Department of Chemistry and Biochemistry, Arizona State University, Tempe, AZ 85287-1604, USA

Received 30 March 2005; received in revised form 14 May 2005; accepted 15 May 2005
Available online 6 July 2005

Abstract

A new high-pressure phase, silicon phosphate hydroxide, was prepared at 8.3 ± 0.5 GPa and 1000 °C in >98% purity. From X-ray diffraction on a pseudo-merohedrally twinned crystal, it was found that $SiPO_4(OH)$ crystallizes in a monoclinic cell with space group $P2_1/n$ (No. 14), $a = 6.8446(11)$ Å, $b = 6.8683(13)$ Å, $c = 6.8446(11)$ Å, $\beta = 119.77(1)^\circ$, and $Z = 4$. The refinement gave a conventional R_{obs} of 0.0320 and wR_{obs} of 0.0864 for the overlapped data from both twin components. In the structure, SiO_6 octahedra form chains along [101], with PO_4 tetrahedra alternating along the chain in the *b*-direction. The parallel chains link up with tetrahedral corners from other chains to form a 3-dimensional network. $SiPO_4(OH)$ belongs to a structural family that includes $HgSeO_4 \cdot H_2O$. It is also related to the $SbOPO_4$ structure by a small distortion that lowers the symmetry from $C2/c$ in $SbOPO_4$ to $P2_1/c$ ($P2_1/n$) in $SiPO_4(OH)$.

Keywords: Silicon phosphates; Six-coordinated silicon; Pseudo-merohedral twinning; High-pressure synthesis

1. Introduction

Various compounds in the binary system P_2O_5–SiO_2 have been reported in the literature, most notably silicon pyrophosphate, SiP_2O_7 (in eight structural polymorphs) [1–5], and silicon orthophosphate, $Si_5O(PO_4)_6$ [6,7]. In the SiP_2O_7 polymorphs, silicon is 6-coordinated, while in $Si_5O(PO_4)_6$ unusual mixed 4,6-coordination is observed. With the exception of naturally-occurring thaumasite, $Ca_3(H_2O)_{12}(Si(OH)_6)(CO_3)(SO_4)$, the silicon phosphates are the only *room pressure* ionic crystalline phases known to possess SiO_6 units. This octahedral coordination extends to several silicophosphate polyanion-bearing compounds, including $(NH_4)_2SiP_4O_{13}$ [8], $Rb_2SiP_4O_{13}$, $Cs_2H_2Si(P_2O_7)_2$, and $BaH_2Si(P_2O_7)_2$ [9].

In general, high pressure promotes densification and higher coordination states. In silicate minerals, such as $MgSiO_3$ enstatite and SiO_2 quartz, SiO_4 tetrahedra assemble at room pressure, whereas SiO_6 octahedra (found in $MgSiO_3$ ilmenite, perovskite, and post-perovskite; SiO_2 stishovite) form at pressures above 8 GPa. A small number of high-pressure silicates display both tetrahedral and octahedral silicon, but this mixed coordination is restricted to pressures between 10 and 30 GPa [10]. A comprehensive review of silicon coordination polyhedra in high-pressure silicates is found in [10].

Since phases within the system P_2O_5–SiO_2 already exhibit 6-coordination at ambient pressure, we thought it appropriate to use these compositions as a basis for exploring pressure-induced coordination changes in silicon. In short, using high pressure, our goal was to force silicon into 7- (or higher) coordination. This coordination is extremely rare; the only apparent example is a ZrO_2-structured form of SiO_2 that has been observed in a meteorite, and for which the structure has not been refined [11]. A target composition for this was $Si_2P_2O_9$, a hypothetical compound that

*Corresponding author. Fax: +1 480 965 2747.
E-mail address: linda.stearns@asu.edu (L.A. Stearns).

0022-4596/$ - see front matter © 2005 Elsevier Inc. All rights reserved.
doi:10.1016/j.jssc.2005.05.030

could have a structure such as that of $Zr_2P_2O_9$, which has Zr in 7-coordination [12].

With every intention of restricting our experiments to P_2O_5–SiO_2-bearing compositions, H_2O inadvertently intruded into the system. As a result, we encountered a new high-pressure phase, $SiPO_4(OH)$, at 8.3 ± 0.5 GPa and 1000 °C. Its crystal structure was elucidated using single crystal X-ray diffraction, the details of which are reported here. $SiPO_4(OH)$ represents the first known high-pressure phase in the system P_2O_5–SiO_2–H_2O; a comprehensive study of phase equilibria in the ternary system was undertaken by Lelong et al. at ambient pressure [13]. While more highly-coordinated silicon eluded us with this attempt, we will continue to pursue new phases at elevated pressures and temperatures.

2. Experimental

2.1. Synthesis

The phosphorus-bearing starting material for all high-pressure runs, $Si_5O(PO_4)_6$, was prepared according to Poojary et al. [6]. The product was repeatedly washed with ethanol and acetone, and its identity and purity confirmed using powder X-ray diffraction. Starting compositions (see Table 1) were encapsulated in annealed Pt tubing and sealed by arc welding. For R-439, it was verified that no water had vaporized from the capsule during arc welding, prior to *P–T* treatment.

High-pressure multi-anvil experiments were conducted in a Walker-style module, using a 14/8 mm assembly [14]. The assembly consisted of an MgO octahedron (14 mm on edge) and WC cubes (8 mm truncations). A graphite furnace with TZM (titanium–zirconium–molybdenum) contacts, MgO spacers, ZrO_2 insulating caps and sleeve, and Pt capsule comprised the internal assembly. A type-S (Pt, Pt-10%Rh) thermocouple entered into the octahedron through mullite and 2-bore Al_2O_3 insulation (cemented to the exterior of the octahedron) and contacted the distal end of the Pt capsule.

The assembly was slowly pressurized to 8.3 ± 0.5 GPa at room temperature, then heated to 1000 °C over the course of an hour. All runs were held at *P–T* for the times indicated in Table 1. Temperature was maintained at 1000 ± 2 °C using a Eurotherm programmable controller, operating on feedback from the thermocouple. Following extended heating at 1000 °C, the runs were quenched by cutting power to the graphite furnace. The temperature dropped to <100 °C in about 5 s. The run products were then recovered to ambient pressure. Powder X-ray diffraction patterns were collected using a Siemens D5000 diffractometer (graphite monochromated Cu$K\alpha$ radiation) with 2θ from 5° to 90°; 0.017° step size, and 1 s/step count time.

2.2. Stoichiometric analysis

A thin section was prepared using grains from R-434 that had been dispersed in a drop of water. A JEOL JXA-8600 electron microprobe, with a 1–3 μm focused beam diameter, 10 nA sample current, and 20 keV accelerating voltage, was utilized for quantitative determination of the composition of all R-434 products. The beam was calibrated using known mineral standards: San Carlos Olivine ($(Mg,Fe)_2SiO_4$) for silicon and apatite ($Ca_5(PO_4)_3$ (F,Cl,OH)) for phosphorous. Apatite was treated as an unknown, and used to verify the accuracy of the calibration. Silicon and phosphorous were measured simultaneously using separate solid-state detectors, while oxygen was calculated directly from the oxides using the data for Si and P.

2.3. Single crystal structural determination

A prismatic, transparent crystal of $SiPO_4(OH)$ from R-434, measuring $100 \times 100 \times 80$ μm, was selected and mounted on a glass fiber for data collection on a Bruker SMART APEX diffractometer with a three-circle goniometer. The diffractometer utilized a 2 K CCD area detector and graphite monochromated Mo$K\alpha$ radiation. Intensity data were collected using SMART v. 5.630 [15] and initial cell parameters were established by centering and indexing 670 reflections from the 1818 frames of the full data set. Using the SAINT v. 6.45A program [16], the frame data were integrated to produce

Table 1
High-pressure experiments at 8.3 ± 0.5 GPa and 1000 °C

Run ID	Starting composition	Duration (h)	Products
R-430	$Si_5O(PO_4)_6$[a]	5.75	$SiPO_4(OH) + SiP_2O_7$
R-434	$Si_5O(PO_4)_6$[a] + 20 wt% SiO_2 quartz	50	$SiPO_4(OH) + SiP_2O_7 + SiO_2$ coesite
R-439	$Si_5O(PO_4)_6 + SiO_2 + H_2O$[b]	33.25	>98% $SiPO_4(OH)$

[a]Starting material contained an unmeasured quantity of molecular and/or physisorbed H_2O. Based on the stoichiometry of Eq. (1), the amount of H_2O in the starting composition is estimated as 4.7 wt%.
[b]Proportions of each reactant according to stoichiometry of Eq. (2).

3835 reflections covering the range in h, k, and l from -10 to 10. The monoclinic unit cell was refined to $a = 6.8446(11)$ Å, $b = 6.8683(13)$ Å, $c = 6.8446(11)$ Å and $\beta = 119.77(1)^\circ$ using 1289 centered reflections. The reduced data were corrected for absorption using Bruker SADABS [17]. Of 1030 independent reflections, 648 were observed according to the criterion $I > 2\sigma(I)$.

The positions of silicon and phosphorous atoms were obtained directly using SHELXS-97 [18], while oxygen and hydrogen atoms were located successively using Fourier difference maps in SHELXL-97 [19]. The structure was refined using full-matrix least squares against F^2 for *all* reflections. In the case of hydrogen, positions were initially determined by difference map and then refined as atoms riding on their bonding partners with restrained distances and thermal parameters. During the refinement, it became evident that the crystal used in data collection was not perfectly single, rather pseudo-merohedrally twinned. This type of twinning is consistent with the near equivalence of lattice parameters a and c [20]. The twin operation $(001, 0\bar{1}0, 100)$ was applied to refine the twin fractions, which further reduced the residuals. The best refinement (i.e., smallest residual) was obtained for space group setting $P2_1/n$ (No. 14), with $R_{obs} = 0.0320$ and $wR_{obs} = 0.0864$. The twin fraction for the minor component refined to 0.1236(13).

It should be noted that the setting $P2_1/n$ was chosen, instead of the more commonly used $P2_1/c$ setting, in order to make the twin relation as simple as possible and in order not to obscure the effects of the twinning, which are discussed further in the results section. The observed cell parameters give rise to concern regarding the higher metric symmetries that are possible for the observed unit cell. Other symmetries considered include hexagonal, orthorhombic, tetragonal, and C-centered monoclinic, none of which provided reasonable solutions to the data set. The internal symmetry of the raw data gives clear indication that the structure is primitive monoclinic rather than other higher symmetries (R_{sym} hexagonal = 0.879, R_{sym} orthorhombic = 0.272, R_{sym} tetragonal = 0.616, R_{sym} C-centered monoclinic = 0.296, R_{sym} primitive monoclinic = 0.018, as provided in SHELXTL XPREP v. 6.12). It should be noted that a solution is obtainable in the space group $C2/c$, but in the final difference maps there are several prominent peaks ($8\,e^-/Å^3$) that appear in unreasonable positions and there are large numbers of strong reflections that disobey the C-centering requirements.

Selected details of the data collection and refinement are provided in Table 2. Further details of the crystal structure investigation can be obtained from the Fachinformationszentrum Karlsruhe, 76344 Eggenstein-Leopoldshafen, Germany, (fax: (49) 7247-808-666; email: crysdata@fiz.karlsruhe.de) on quoting the depository number CSD #415271.

Table 2
Crystallographic parameters for $SiPO_4(OH)$

Formula	H O5 P Si
FW	140.07
Cell setting	Monoclinic
Space group	$P2_1/n$ (No. 14)
Crystal size (μm)	100 × 100 × 80
Color	Transparent
a (Å)	6.8446(11)
b (Å)	6.8683(13)
c (Å)	6.8446(11)
β (deg)	119.77(1)
V (Å^3)	279.30(8)
Z	4
D_x (Mg/m^3)	3.331
$F_0(000)$	280
μ (mm^{-1})	1.265
Diffractometer	Bruker SMART APEX [9]
T (K)	298 (2)
Radiation type	Mo$K\alpha$ ($\lambda = 0.71073$ Å) Graphite monochromated
Measurement method	ω scan
$(h,k,l)_{min}, (h,k,l)_{max}$	$-10, 10$
No. of measured reflections	3835
No. of unique data, R_{int}	1030, 0.0445
No. of observed reflections	648
Observed criterion	$>2\sigma(1)$
Adsorption correction details	Empirical, Bruker SADABS [11]
Min. max transmission	0.8275, 0.9985
Max. full coverage fraction	0.955, 0.955
θ_{full}	33.32
Refined method	Full-matrix least squares[a] on F^2
Extinction correction method	SHELXL [13]
Extinction coefficient	0.012(4)
Extinction expression	$F_c^* = kF_c[1 + 0.001 \times F_c^2\lambda^3/\sin(2\theta)]^{-1/4}$
No. of reflections used in l.s. derivatives	1030
No. of parameters refined	66
R_{obs}, R_{all}	0.0320, 0.0522
wR_{obs}, wR_{all}	0.0864, 0.0916
Goodness of fit, S	1.117
$(\Delta\rho)_{max}, (\Delta\rho)_{min}$ (e/Å^3)	0.614, −0.489
RMS (e/Å^3) in final difference map	0.121

[a] $w = 1/[\sigma^2(F_o^2) + (0.0349P)^2 + 0.0886P]$, where $P = (F_o^2 + 2F_c^2)/3$.

3. Results and discussion

In the course of arriving at the new material, two principal reactions were investigated:

$$Si_5O(PO_4)_6 + 2H_2O = SiP_2O_7 + 4SiPO_4(OH), \quad (1)$$

$$Si_5O(PO_4)_6 + SiO_2 + 3H_2O = 6SiPO_4(OH). \quad (2)$$

In R-430 and R-434, the starting compositions were $Si_5O(PO_4)_6$ (R-430) and $Si_5O(PO_4)_6 + 20$ wt% SiO_2

(R-434). Following P–T treatment, and rapid thermal quenching, run products were analyzed using powder X-ray diffraction. A mixture of cubic SiP_2O_7, SiO_2 (coesite), and an unknown phase was observed in both run products (see Table 1). The ratio of SiP_2O_7 to the unknown phase was identical for R-430 and R-434, despite different starting compositions and heating durations (6 h for R-430 vs. 50 h for R-434). This led us to conclude that formation of the new phase was not kinetically hindered. After the composition of the unknown, $SiPO_4(OH)$, was established by X-ray diffraction on a single crystal from R-434, and the intrusion of H_2O into the system was confirmed, it became clear that H_2O was limiting the yield of the new phase in R-430 and R-434 starting compositions. A new run (R-439) was prepared, containing $Si_5O(PO_4)_6$, SiO_2, and deionized liquid water in the stoichiometric proportions defined by Eq. (2). The product was >98% $SiPO_4(OH)$, as confirmed by powder X-ray diffraction (Fig. 1). This pattern was not fitted with a Rietveld refinement because the material exhibited strong preferred orientation.

The introduction of H_2O into the system can be attributed to a hygroscopic gel, amorphous $Si_5O(PO_4)_6$, a byproduct of the synthesis of crystalline material of the same composition. PXRD on the starting material showed a small amorphous background, consistent with this interpretation. Residual water may also have been introduced via crystalline $Si_5O(PO_4)_6$, which, according to TGA experiments of Poojary et al. [6], contained adsorbed and chemically-bound water amounting to 2% by weight. Based on the stoichiometry of Eq. (1), the amount of H_2O present in the R-430 and R-434 starting compositions was 4.7 wt%.

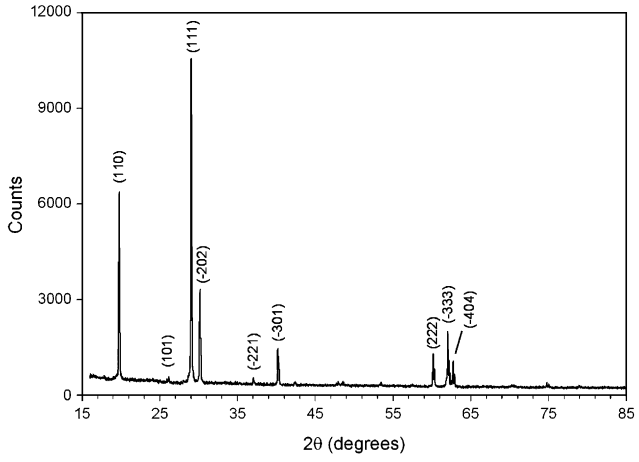

Fig. 1. Powder X-ray diffraction pattern for >98% $SiPO_4(OH)$.

Quantitative electron microprobe analysis (for results, see Table 3) was used to confirm the stoichiometry of the new phase: $SiPO_4(OH)$. The wt% contributions of Si, P, and O do not total 100%, owing to the fact that the hydroxyl group could not be quantified directly using the wavelength-dispersive X-ray technique. Based on the stoichiometry of Eq. (2), the amount of oxygen and hydrogen deriving from hydroxyl are calculated as 5.71 and 0.72 wt%, respectively. The total wt% for $SiPO_4(OH)$ increases to 93.23 wt% when these values are included. We observed that the new phase is sensitive to the electron beam (small holes appeared in the grain where the beam had been directed), which might explain the low total. Since the other phases, SiP_2O_7 and SiO_2, did not exhibit any such sensitivity, we attribute this behavior to the presence of a hydroxyl group in the structure. The OH is further corroborated by single crystal X-ray diffraction: hydrogen atoms were located in Fourier difference maps during structure solution, and are consistent with the overall charge balance and idealized stoichiometry of the phase.

3.1. Crystal structure of $SiPO_4(OH)$

As summarized in Table 2, $SiPO_4(OH)$ crystallizes in a monoclinic cell, with $a = 6.8446(11)$ Å, $b = 6.8683(13)$ Å, $c = 6.8446(11)$ Å and $\beta = 119.77(1)^\circ$. The space group is $P2_1/n$ (No. 14). Positional and thermal parameters for all atoms are listed in Tables 4 and 5. The contents of a unit cell are shown in Fig. 2.

The primary building block of the structure is a pair of corner-sharing SiO_6 octahedra and a PO_4 tetrahedron, which connect into a 3-ring. The octahedra form chains along [101], with the tetrahedra alternating along

Table 3
Composition (wt%) of R-434 products as determined by electron microprobe

Phase	Si (wt%)	P (wt%)	O (wt%)	Total (wt%)
$SiPO_4$ (OH)	18.55 ± 0.58	20.56 ± 0.83	47.69 ± 1.23[a]	86.80 ± 2.22[b]
Ideal	(20.05)	(22.11)	(57.11)	
SiO_2	45.79 ± 1.02	0.04 ± 0.07	52.21 ± 1.06	98.04 ± 2.01
Ideal	(46.74)	(0.00)	(53.26)	
SiP_2O_7	13.74 ± 0.72	28.95 ± 1.53	53.04 ± 2.32	95.73 ± 4.16
Ideal	(13.90)	(30.66)	(55.44)	

Errors are reported as $\pm 2\sigma$. Ideal compositions for the indicated stoichiometries are given in parentheses.
[a]Does not include oxygen from H_2O component.
[b]Does not include oxygen and hydrogen from H_2O, which amount to 5.71 wt% (O) and 0.72 wt% (H), as calculated from Eq. (2).

the chain in the *b*-direction (Fig. 3). The chains link up with tetrahedral corners from other chains, to form a 3-dimensional network.

In the coordination octahedron (Fig. 4), silicon is bonded to six oxygen atoms, four of which derive from PO_4 tetrahedra and two from SiO_6 octahedra. Bond lengths range from 1.706 to 1.815 Å and bond angles from 86.63 to 93.53° (Table 6), and are consistent with those found in the silicon phosphates SiP_2O_7 [1–5] and $Si_5O(PO_4)_6$ [6]. Using mean quadratic elongation (QE) as a measure of distortion [21], the octahedra can be described as fairly regular with QE = 1.0018 (QE = 1 for the ideal, undistorted configuration). The PO_4 tetrahedra also show slight distortion (QE = 1.0025), with bond lengths ranging from 1.507 to 1.548 Å and bond angles from 103.58 to 111.57°.

From a crystal chemical standpoint, the OH species in the structure should be O(2), which is the bridging oxygen between two SiO_6 octahedra, because this atom is underbonded. Each of the Si neighbors contributes only about 2/3 to the bond sum. This is also consistent with a peak in the difference map of the structure without hydrogen, about 1 Å away from O(2). When hydrogen is refined with a fixed bond length to O(2), the location indicates that the hydrogen forms a bifurcated hydrogen bond with two oxygen atoms on the neighboring PO_4 tetrahedron, O(3) and O(4), with a strong preference for O(4). The O(2)–O(3) and O(2)–O(4) distances are 2.52 and 2.53 Å, consistent with weak hydrogen bonding such as that observed in brucite ($Mg(OH)_2$).

$SiPO_4(OH)$ is, excluding the hydrogen atoms, isostructural with $HgSeO_4 \cdot H_2O$ [22] and a small family of other compounds. These compounds crystallize in the space group $P2_1/c$ ($P2_1/n$) and are characterized by chains of octahedra that are bridged by tetrahedra which share opposing pairs of corners with the chains, such that each tetrahedron is linked to two of the chains. This structure was in turn assigned to a larger family of structures that have different numbers of chains linked to each tetrahedron [23].

Another related structure is that of $SbOPO_4$ [24], which crystallizes in the space group $C2/c$. Excluding the hydrogen atom in the current structure, the $SbOPO_4$ structure has the same topology, and may be considered the aristotype example of the structural family because it has the highest symmetry that is intrinsic to this particular linkage of octahedra and tetrahedra. However, in the current structure, as in all the structures of the $HgSeO_4 \cdot H_2O$ series, there is a lowering of

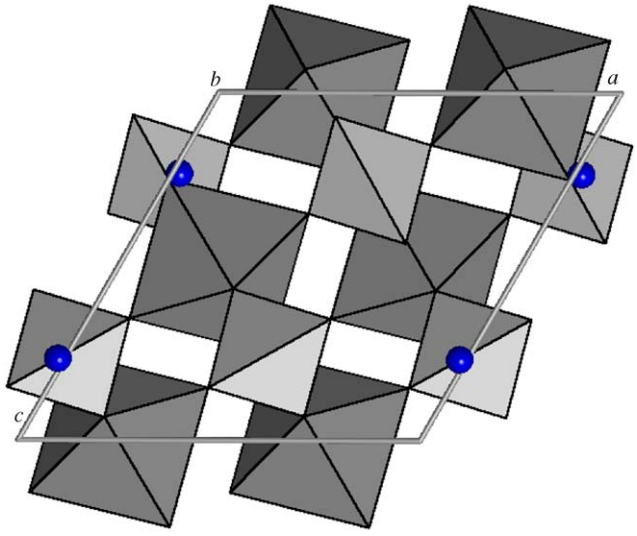

Fig. 2. Polyhedral representation of $SiPO_4(OH)$: view of the *a*–*c* plane, which appears nearly metrically hexagonal. SiO_6 octahedra (darker), PO_4 tetrahedra (lighter), and hydrogen atoms (circles) are shown.

Table 4
Atomic coordinates and equivalent isotropic thermal parameters (Å^2)

Atom	Site	*X*	*Y*	*Z*	U_{eq}[a]
P	4e	1.0009(2)	0.37843(8)	0.2519(2)	0.00420(15)
Si	4e	0.7492(2)	0.7472(2)	0.0001(2)	0.00447(16)
H	4e	0.5184	0.5503	−0.2663	0.007
O(1)	4e	0.8186(5)	0.5082(4)	0.0659(5)	0.0073(6)
O(2)	4e	0.4981(6)	0.6654(2)	−0.2499(5)	0.0062(3)
O(3)	4e	0.8976(4)	0.2411(4)	0.3493(4)	0.0074(5)
O(4)	4e	1.1032(4)	0.2418(4)	0.1512(4)	0.0062(5)
O(5)	4e	1.1771(5)	0.5068(4)	0.4315(5)	0.0057(6)

[a] U_{eq} calculated as $(\Sigma_i\Sigma_j U_{ij} a^i a^j a_i a_j)/3$.

Table 5
Anisotropic thermal parameters (Å^2)

Atom	U_{11}	U_{22}	U_{33}	U_{23}	U_{13}	U_{12}
P	0.0040(3)	0.0046(3)	0.0040(3)	−0.0008(5)	0.00198(19)	−0.0011(5)
Si	0.0046(3)	0 0045(3)	0.0042(3)	0.0004(2)	0.0021(2)	0.0006(2)
O(1)	0.0054(13)	0.0065(14)	0.0068(13)	−0.0001(10)	0.0007(11)	−0.0016(10)
O(2)	0.0069(7)	0.0033(7)	0.0056(7)	0.0006(12)	0.0009(6)	−0.0011(13)
O(3)	0.0069(13)	0.0115(13)	0.0063(13)	−0.0016(11)	0.0053(11)	−0.0020(13)
O(4)	0.0080(13)	0.0035(12)	0.0089(13)	−0.0011(10)	0.0056(11)	0.0004(12)
O(5)	0.0053(13)	0.0050(13)	0.005(12)	−0.0015(10)	0.0016(11)	−0.0032(10)

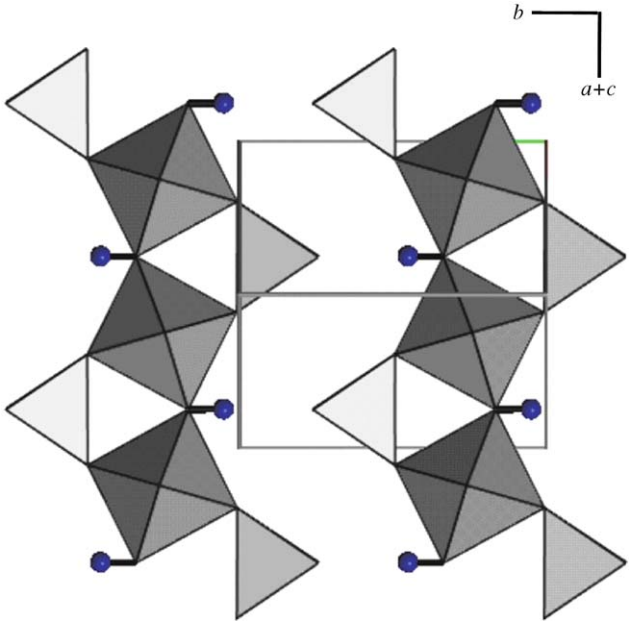

Fig. 3. View of the structure down ($\bar{1}01$), emphasizing the chains of SiO_6 octahedra with PO_4 tetrahedra bridging their corners. Hydrogen atoms are also shown (circles).

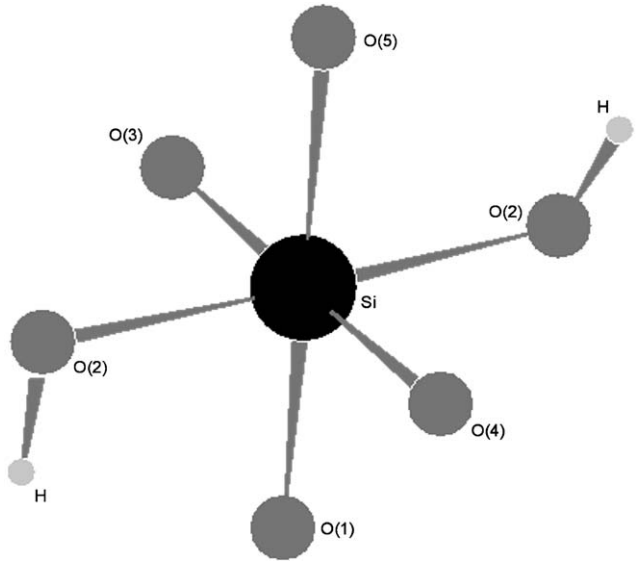

Fig. 4. Coordination polyhedron around silicon. SiO_6 octahedra are bridged by O(2), and PO_4 tetrahedra by O(1), O(3), O(4), and O(5).

symmetry from $C2/c$ to $P2_1/c$ ($P2_1/n$). Because the departure from $C2/c$ symmetry is very small (the departures of the atom locations from their ideal positions are smaller than the uncertainties for all the atoms), it is worth discussing in more detail. In the case of $HgSeO_4 \cdot H_2O$ [22] (which was studied by neutron diffraction), the orientation of the H_2O molecule was an important factor in breaking the symmetry from the $SbOPO_4$ aristotype. We propose that the current case, which is the first example of a hydroxide with this structure, behaves similarly with respect to the H atom. In order for this structure to have $C2/c$ symmetry, both O(2) and the hydrogen atom bonded to O(2) would have to lie on the 2-fold axis. We hypothesize that the primary symmetry-breaking is the motion of the hydrogen atom off the 2-fold axis of $C2/c$, lowering it to a 2_1-axis. This would happen if the OH-group is oriented preferentially toward one of the two next-neighbor oxygen atoms. Such preferential orientation of hydrogen is very common in structures studied by neutron diffraction. In our refinement, the difference peak that we identified as the hydrogen atom is indeed off the 2-fold axis, and is directed towards O(4) and away from O(3), as already mentioned. However, because of the weak scattering of hydrogen, neutron diffraction measurements would be needed to provide definitive proof of this symmetry-breaking by the hydrogen.

The lattice parameters show a high degree of metric pseudo-symmetry. Although the structure itself does not appear to have any hexagonal aspect to it (for example, there is no *hcp* packing of anions), the *a*–*c* plane is nonetheless nearly metrically hexagonal. The *b* parameter is also very similar to the *a* and *c* parameters. These near coincidences appear to have to do with the Si–O and P–O bond lengths and the particular structural packing. The lattice parameters may be expressed for ideal polyhedra in terms of the octahedral and tetrahedral bond lengths, l_o and l_t. Given that the Si–O bond length in an octahedron should be about 1.768 Å and the P–O tetrahedral bond length about 1.519 Å ($l_o/l_t = 1.164$), the expected lattice parameters are $a = 6.822$ Å, $b = 6.919$ Å, $c = 6.916$ Å, $\beta = 119.5°$. A β angle of exactly 120° would occur for $l_o/l_t = 1.25$, the coincidence $c = b$ would occur when $l_o/l_t = 1.16$; $a = b$ when $l_o/l_t = 1.20$, and $a = c$ when $l_o/l_t = 1.26$. Thus it appears to be a structural coincidence that $a \sim b \sim c$ and $\beta \sim 120°$, although the structure itself is strongly monoclinic. A broader view of the structural packing is shown in Fig. 5, in which a pseudo-orthorhombic supercell is clearly visible, along with the monoclinic unit cell with a β angle of nearly 120°.

The similarity between *a* and *c* is consistent with the tendency for twinning, as shown by the presence of pseudo-merohedral rotational twins about (110) (relating *a* and *c*) that were encountered during the structure solution. This type of twinning has been observed previously by Yang et al. in monoclinic crystals having nearly equal *a* and *c* axes [20]; those authors showed how the resulting *a* and *c* parameters are indistinguishable in the refinement, which is also consistent with our observation of apparently identical *a* and *c* parameters, including the standard deviations. Basically, the overlap between spots due to twinning is so strong that *a* and *c* are fitted using the same set of spots, and are thus refined

Table 6
Selected interatomic distances (Å) and bond angles (deg)

PO_4 tetrahedra					
P–O(1)	1.548(3)	O(1)–P–O(3)	110.99(16)	O(3)–P–O(5)	111.36(16)
P–O(3)	1.517(3)	O(1)–P–O(4)	110.25(16)	O(4)–P–O(5)	111.57(16)
P–O(4)	1.525(3)	O(1)–P–O(5)	109.02(9)		
P–O(5)	1.507(3)	O(3)–P–O(4)	103.58(9)		
SiO_6 octahedra					
Si–O(1)	1.706(3)	O(1)–Si–O(2)	93.53(14)	O(2)–Si–O(5)	86.63(13)
Si–O(2)	1.815(3)	O(1)–Si–O(2′)	87.7	O(2′)–Si–O(3)	89.8
Si–O(2′)	1.810(3)	O(1)–Si–O(3)	89.28(15)	O(2′)–Si–O(4)	90.6
Si–O(3)	1.762(3)	O(1)–Si–O(4)	91.76(14)	O(2′)–Si–O(5)	92.1
Si–O(4)	1.771(3)	O(1)–Si–O(5)	179.8(2)	O(3)–Si–O(4)	178.91(19)
Si–O(5)	1.757(3)	O(2)–Si–O(2′)	178.7	O(3)–Si–O(5)	90.74(15)
		O(2)–Si–O(3)	89.84(16)	O(4)–Si–O(5)	88.22(14)
		O(2)–Si–O(4)	89.79(15)		
P–O(1)–Si	140.94(19)	P–O(4)–Si	139.57(18)	Si–O(2)–Si	142.6
P–O(3)–Si	140.19(19)	P–O(5)–Si	141.75(19)		

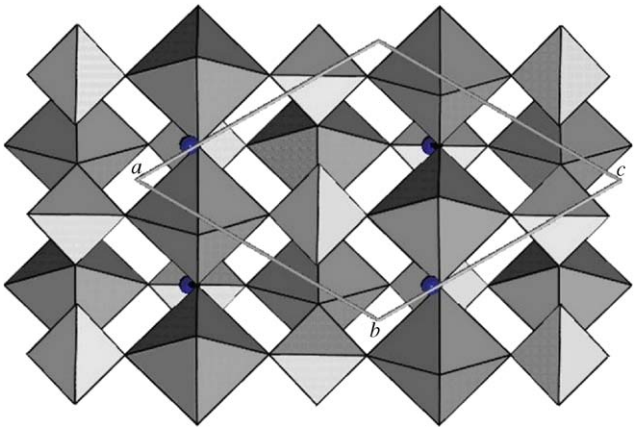

Fig. 5. Broader view of the $SiPO_4(OH)$ structure showing a nearly metrically orthorhombic supercell (represented by all the polyhedra shown) along with the monoclinic primitive unit cell. The overall linkage of the structure is most clearly visible in this view.

as equal in *d*-spacing. However, because the two twin fractions are non-equal, the structure can still be extracted from the data. The "identical" *a* and *c* parameters also lead to a metrically orthorhombic supercell; however, the symmetry of the linkage of octahedra and tetrahedra is monoclinic as described above.

The twinning could indicate a partially converted phase, and thereby thermodynamic metastability of the material. It is possible that the structure was $C2/c$ at the pressure and temperature condition of the experiment, but converted to $P2_1/c$ ($P2_1/n$) during quenching or decompression, perhaps by motion of the hydrogen atoms off of the 2-fold axis. The observed twin law is consistent with such a transition. This possible phase transition would be best investigated with an independent in situ experiment, particularly neutron diffraction at HP-HT.

Finally, we mention that the $C2/c$ aristotype of the current structure is isosymmetric (*i.e.*, has the same space group and Wyckoff sites) with $CaCrF_5$ [25,26], which has Ca in 7-coordination and Cr in 6-coordination. If a structural pathway is available, this would provide a potential technique for raising the coordination numbers of both Si and P, by direct compression of $SiPO_4(OH)$. A compression study of this material would be warranted to look for such a transition.

4. Acknowledgments

The authors wish to thank Gordon Moore for providing training and assistance on the electron microprobe. We also acknowledge Darren Locke for several useful discussions. The synthesis, crystal structure determination, and microprobe studies were carried out with the support of Award NSF EAR-0074089 to KL. We would like to express our gratitude to the National Science Foundation for their contribution toward the purchase of the single crystal instrumentation used in this study through Award NSF CHE-9808440.

References

[1] D.M. Poojary, R.B. Borade, F.L. Campbell III, A. Clearfield, J. Solid State Chem. 112 (1994) 106.
[2] H. Markart, Helv. Chim. Acta 50 (1967) 399.
[3] G. Bissert, F. Liebau, Acta Crystallogr. B 26 (1970) 233.
[4] F. Liebau, K.F. Hesse, Z. Kristallogr. 133 (1971) 213.
[5] E. Tillmans, W. Gebert, W.H. Baur, J. Solid State Chem. 7 (1973) 69.
[6] D.M. Poojary, R.B. Borade, A. Clearfield, Inorg. Chim. Acta 208 (1993) 23.
[7] H. Mayer, Monatsh. Chem. 105 (1974) 46.

[8] A. Durif, J.C. Guitel, M.T. Averbuch-Pouchot, Acta Crystallogr. B 52 (1976) 2957.
[9] K. Königstein, M. Jansen, Chem. Ber. 127 (1994) 1213.
[10] L.W. Finger, R.M. Hazen, Acta Crystallogr. B 47 (1991) 561.
[11] A. El Goresy, L. Dubrovinsky, T.G. Sharp, S.K. Saxena, M. Chen, Science 288 (2000) 1632.
[12] W. Gebert, E. Tillman, Acta Crystallogr. B 31 (1975) 1768.
[13] B. Lelong, A. Boulle, Compt. Rend. 255 (1962) 530.
[14] K. Leinenweber, J. Parise, Am. Mineral. 82 (1997) 475.
[15] SMART: Program for collecting single crystal X-ray diffraction data from 2-dimensional detectors, Bruker Analytical X-Ray Instruments, Inc., Madison, 2001.
[16] SAINT: Program for integrating single crystal X-ray diffraction data from 2-dimensional detectors, Bruker Analytical X-Ray Instruments, Inc., Madison, 2001.
[17] R.H. Blessing, Acta Crystallogr. A 51 (1995) 33.
[18] G.M. Sheldrick, Acta Crystallogr. A 46 (1990) 467.
[19] G.M. Sheldrick, SHELXS97 and SHELXL97, University of Göttingen, Göttingen, 1997.
[20] F. Yang, Z. Dauter, A. Wlodawer, Acta Crystallogr. D 56 (2000) 959.
[21] K. Robinson, G.V. Gibbs, P.H. Ribbe, Science 172 (1971) 567.
[22] C. Stålhandske, Acta Crystallogr. B 34 (1978) 1408.
[23] O. Bars, J.Y. Le Maroille, D. Grandjean, Acta Crystallogr. B 37 (1981) 2143.
[24] Y. Piffard, S. Oyetola, A. Verbaere, M. Tournoux, J. Solid State Chem. 63 (1986) 81.
[25] D. Dumora, R. Von der Muhll, J. Ravez, Mat. Res. Bull. 6 (1971) 561.
[26] K.K. Wu, I.D. Brown, Mat. Res. Bull. 8 (1973) 593.